© 2017. Published by The Company of Biologists Ltd | Development (2017) 144, 3241-3252 doi:10.1242/dev.150904

RESEARCH ARTICLE

Endothelial cells respond to the direction of mechanical stimuli through SMAD signaling to regulate coronary artery size

Aruna Poduri[1], Andrew H. Chang[1,2], Brian Raftrey[1], Siyeon Rhee[1], Mike Van[1] and Kristy Red-Horse[1,*]

ABSTRACT

How mechanotransduction intersects with chemical and transcriptional factors to shape organogenesis is an important question in developmental biology. This is particularly relevant to the cardiovascular system, which uses mechanical signals from flowing blood to stimulate cytoskeletal and transcriptional responses that form a highly efficient vascular network. Using this system, artery size and structure are tightly regulated, but the underlying mechanisms are poorly understood. Here, we demonstrate that deletion of *Smad4* increased the diameter of coronary arteries during mouse embryonic development, a phenotype that followed the initiation of blood flow. At the same time, the BMP signal transducers SMAD1/5/8 were activated in developing coronary arteries. In a culture model of blood flow-induced shear stress, human coronary artery endothelial cells failed to align when either BMPs were inhibited or *SMAD4* was depleted. In contrast to control cells, *SMAD4*-deficient cells did not migrate against the direction of shear stress and increased proliferation rates specifically under flow. Similar alterations were seen in coronary arteries *in vivo*. Thus, endothelial cells perceive the direction of blood flow and respond through SMAD signaling to regulate artery size.

KEY WORDS: SMAD signaling, Coronary artery, Shear stress, Endothelial cells, Cell migration

INTRODUCTION

Mechanical signals are an integral component of tissue development and homeostasis, in which they can influence cell behavior by inducing structural and transcriptional changes. However, we are only beginning to understand how mechanosensing and transcriptional regulation intersect to influence organogenesis (Fernandez-Sanchez et al., 2015). Endothelial cells that line blood vessels are good models for studying this process because they use the mechanical signals of flowing blood to shape development of the vasculature. Endothelial cells are able to sense small variations in the direction, magnitude and regularity of blood flow-induced shear stress (Givens and Tzima, 2016; Wang et al., 2013), and respond by directing vasculature remodeling (Baeyens et al., 2016a; Culver and Dickinson, 2010). Specifically, endothelial cells of the embryonic vascular plexus can detect whether their vessel is receiving high, low or irregular fluid flow and initiate morphogenic programs that create the most efficient pathway for blood. In the adult, if a vessel experiences too high or too low levels of blood flow, their endothelial cells will begin a program to either increase or decrease its diameter, respectively. These adaptive mechanisms are critical for a well-functioning cardiovascular system, but their underlying mechanisms are poorly understood (Dolan et al., 2013).

In arterial blood vessels, shear stress is high and laminar (i.e. invariable and parallel to the vessel wall) causing endothelial cells to align parallel to the direction of flow and express arterial-specific genes (Culver and Dickinson, 2010; Givens and Tzima, 2016). This effect on endothelial cells is specific to arterial-type shear stress as shown by *in vitro* and *in vivo* experiments. Cultured cells do not align or properly induce arterial genes when exposed to low or oscillatory flow. Similarly, endothelial cells at artery branch points and curves, where flow is disturbed and irregular, are not aligned (Chiu and Chien, 2011). The nonaligned phenotype correlates with disease susceptibility as atherosclerotic plaques develop specifically at branch points and curves (Nakashima et al., 1994). Cells at these locations also preferentially express proinflammatory, proatherogenic molecules (Hahn and Schwartz, 2009; Hajra et al., 2000). Thus, understanding how endothelial cells sense and respond to flow direction could increase our understanding and facilitate treatment of important human vascular pathologies.

Recent studies have revealed that the bone morphogenetic protein (BMP) pathway is important for flow-induced responses, and that receptor activation can be stimulated and/or modulated by shear stress (Baeyens et al., 2016b; Zhou et al., 2012). Specifically, expression of the BMP receptor activin receptor-like kinase 1 (Alk1 – Acvrl1, Zebrafish Information Network) is upregulated by shear stress in zebrafish and binds to BMP10 in the blood to induce arterial quiescence, which limits artery size and suppresses arterial-venous malformations (Corti et al., 2011; Laux et al., 2013). In mice, flow potentiates BMP9/10-induced signaling, which is dependent on its co-receptor endoglin (Eng) (Baeyens et al., 2016b). Interestingly, there is evidence that SMAD1/5/8 activation downstream of BMP receptors can be induced by flow in the absence of ligand, suggesting a direct reaction of the receptors to mechanotransductive forces (Zhou et al., 2012). These mechanisms are particularly significant because the vast majority of cases of hereditary hemorrhagic telangiectasia (HHT), which is a disease characterized by pathological arterial-venous malformations (AVMs), are associated with mutations in *ALK1*, *ENG* or *SMAD4* (Dupuis-Girod et al., 2010; McDonald et al., 2015). Thus, understanding how the BMP/SMAD pathway influences endothelial responses to flow to impact vessel development is an important goal.

Here, we demonstrate that the transcription factor SMAD4 is critical for establishing proper coronary artery size during mouse embryonic development, through mediating endothelial cell responses guided by the direction of blood flow. *Smad4* deletion dramatically increased coronary artery size, a phenotype that arose

[1]Department of Biology, Stanford University, Stanford, CA 94305, USA. [2]Department of Developmental Biology, Stanford University, Stanford, CA 94305, USA.

*Author for correspondence (kredhors@stanford.edu)

A.P., 0000-0002-1698-7167; K.R.-H., 0000-0003-1541-601X

Received 22 February 2017; Accepted 22 July 2017

Development (2017) 144, 3241-3252 doi:10.1242/dev.150904

following the establishment of coronary blood flow, and blood flow initiation coincided with SMAD1/5/8 activation. *In vitro*, *SMAD4* depletion in human coronary artery endothelial cells, or BMP inhibition, completely blocked their ability to align. *SMAD4* knockdown prevented cell migration against the direction of flow, but only mildly affected polarization against flow and random migration. In addition, *SMAD4* knockdown cells increased their proliferation in the presence of flow, indicating that SMAD4 functions to restrain flow-activated proliferative signals. Both less robust alignment and increased proliferation also occurred in mutant coronary arteries. These data show that inhibiting SMAD4 signaling disrupts flow-directed cell behaviors resulting in nonlethal increases in coronary artery size, which could be explored as a method to increase blood flow during cardiac repair.

RESULTS

Smad4 depletion leads to progressive dilation of coronary arteries

To identify pathways that might lead to therapeutic increases in coronary artery size, we assessed the effects of deleting important developmental genes on coronary artery development. Deletion of the transcription factor *Smad4* directly preceding coronary angiogenesis to block signaling downstream of all TGFβ and BMP receptors had profound effects, specifically on arterial vessels. We initially deleted *Smad4* in all cells by administering tamoxifen to mouse embryos containing the *RosaCreER* and *Smad4* floxed alleles at embryonic day (E) 10.5 and E11.5. Western analysis of embryo lysates showed depletion of SMAD4 protein (Fig. S1A). *Smad4* deletion did not significantly affect heart size (Fig. 1A,B), vascular plexus migration to the heart (Fig. 1A,C), or intramyocardial capillary density and branching (Fig. 1D,E). Peritruncal vessels were also normal (Fig. S1B,C). Thus, with our genetic deletion protocol, early coronary angiogenesis did not require SMAD signaling.

In contrast to apparently normal angiogenesis, arterial development in *Smad4*-deficient animals was dramatically disrupted. The first abnormalities were observed in mutant hearts at E13.5, when large dilations in the right (Fig. 1F) and left (Fig. S2A,B) coronary artery stems proximal to the aorta were found. This is the time point just after the developing coronary plexus attaches to the aorta to establish blood flow. Initially, arterial dilations were restricted to the region of the vascular plexus near the aortic attachment (Fig. 1G, E13.5). However, at later time points, the increase in lumen diameter over controls had spread first to middle regions of the artery at E14.5 and then to distal portions at E15.5 (Fig. 1G,H; E14.5 and E15.5). Vascular smooth muscle cells were present around arteries as assessed by smooth muscle-myosin heavy chain (SM-MHC) immunostaining (Fig. 1H and Fig. S1D). Quantifying arterial coverage by SM-MHC showed that there were no significant differences, either around the coronary artery or the aorta (Fig. 1I,J). No significant changes were observed in coronary veins at the time point studied (E15.5) (Fig. S3A,B). We concluded that within the developing coronary vasculature, SMAD signaling is dispensable for normal vascular plexus expansion and initial capillary development, but is required for restricting artery size following the onset of blood flow.

We next used a more selective Cre line to investigate in which cells SMAD4 is functioning during artery development. We use *ApjCreER*, which is heavily expressed in veins and many angiogenenic vessel beds (Chen et al., 2014). Therefore, in the heart, it would most efficiently delete *Smad4* in the sinus venosus and sinus venosus-derived coronary vessels. Endothelial *Smad4* deletion (via administration of tamoxifen at E10.5 and E11.5) resulted in the same dilated artery phenotype as seen with *RosaCreER*-induced deletion (Fig. 1G). It was important to investigate whether structural defects in the heart could be a primary cause of the arterial phenotype. We found that *Smad4* deletion with *RosaCreER* had no effect on the diameters of the aortic lumen (Fig. S3C), sinotubular junction (Fig. S3D) and aortic leaflets (Fig. S3E). Together, these data are consistent with a coronary endothelial cell autonomous function for SMAD4 during artery development.

SMAD1/5/8 is activated in coronary arteries through the onset of blood flow

SMAD4 is required for transcriptional changes downstream of both TGFβ and BMP signals by associating with SMAD2/3 or SMAD1/5/8, respectively. We were able to assess the SMAD1/5/8 arm of the pathway using an antibody that recognizes the phosphorylated, activated form of these proteins in whole mount immunofluorescence. Imaging coronary vessels near the aorta directly before connection to the aorta (E12.5) detected little to no phosphorylated SMAD1/5/8 (Fig. 2A). However, activated SMAD1/5/8 was abundant in coronary artery stems and downstream vessels at E13.5 after the establishment of blood flow (Fig. 2A). SMAD1/5/8 was also phosphorylated in endothelial cells of the capillary plexus and arterial remodeling zone within the ventricle at E13.5 (Fig. 2B, E13.5). SMAD1/5/8 continued to be activated in developing arteries and plexus/capillary cells, but was significantly decreased in mature arteries (Fig. 2B,C; E17.5). Reagents to assess SMAD2/3 were not robust; thus, activation of this pathway cannot be excluded in our studies. In summary, activation of the SMAD1/5/8 complex in coronary endothelial cells is coincident with artery growth in response to blood flow; it is induced following aortic attachment but decreases again as the vessels mature.

Because activated SMAD1/5/8 was decreased in more mature arteries, we tested whether removing *Smad4* after the activation window affected artery size. Tamoxifen was administered at E15.5 and E16.5 to the *RosaCreER, Smad4* floxed line. Embryos were collected at E18.5 and artery diameters were measured. In contrast to the dramatic effect with earlier deletion, artery sizes were similar among control and mutant animals (Fig. 2D). These data support a model in which SMAD signaling functions in the few days following the onset of blood flow to restrict artery size, and that it does so, at least in part, by activating SMAD1/5/8.

In vitro, *SMAD4*-depleted cells do not align and increase proliferation in response to shear stress

To better understand how SMAD signaling influences coronary artery size following the onset of blood flow, we used *in vitro* systems to investigate its effects on endothelial cell behavior under shear stress. Primary human coronary artery endothelial cells (HCAECs) were depleted of *SMAD4*, which resulted in an average 80% decrease in the number of *SMAD4* transcripts (Fig. 4G). The cells were exposed to shear stress conditions, and different cellular parameters were assessed. Our first observation was that, in contrast to control cells, *SMAD4*-depleted HCAECs did not align parallel to flow when exposed to 24 h shear stress using orbital rotation (Dardik et al., 2005; dela Paz et al., 2012) (Fig. S4A). Measuring cell length versus width revealed that as the control cells elongated, *SMAD4* knockdown cells did not efficiently elongate in response to flow (Fig. S4B). Identical results were obtained when cells were cultured in a laminar flow chamber and exposed to 35 dynes/cm^2 (Fig. 3A,B). Thus, SMAD4 signaling is involved in the cell shape changes induced by blood flow.

We next aimed to understand why alignment was defective under SMAD4 knockdown conditions. There are at least two possible

Development (2017) 144, 3241-3252 doi:10.1242/dev.150904

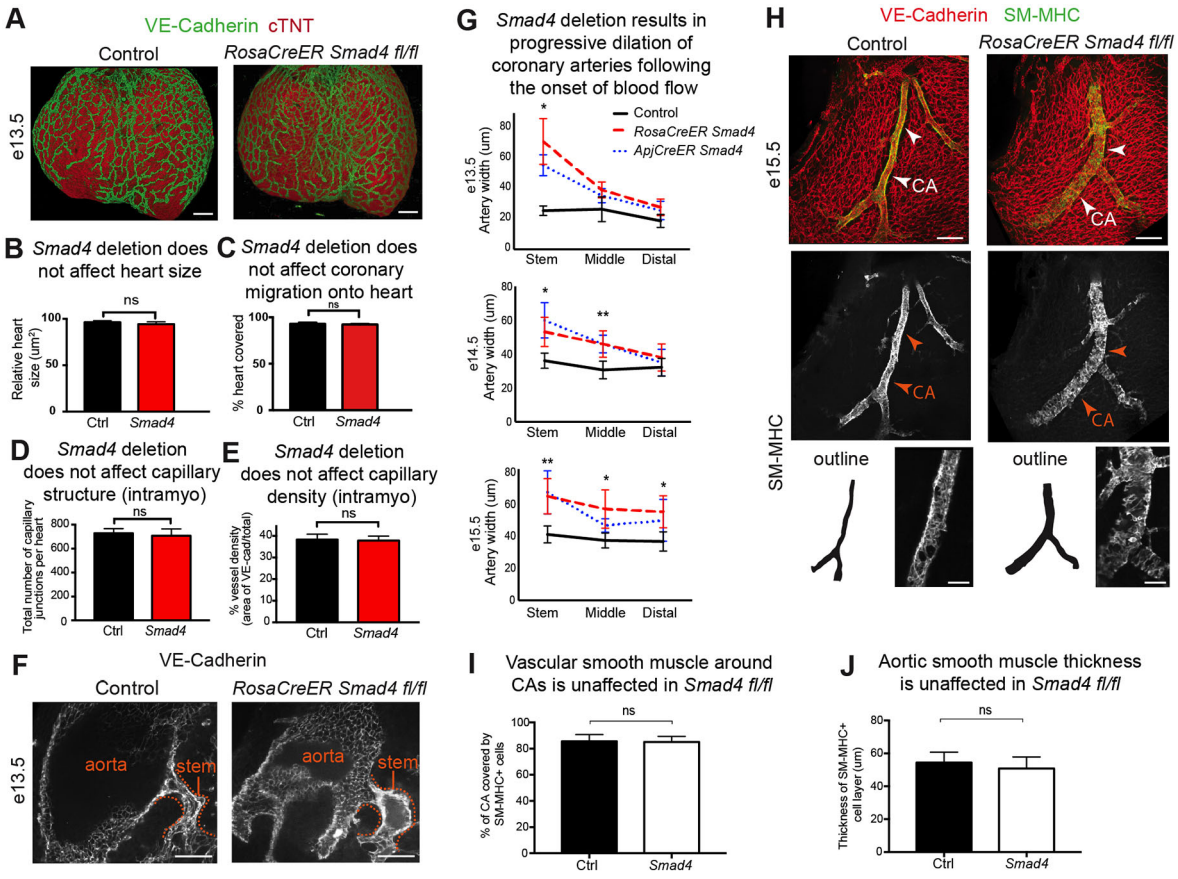

Fig. 1. *Smad4* deletion increases coronary artery size in the developing heart. (A) Confocal images of the dorsal side of the heart immunostained for endothelial cells (green) and cardiac muscle (red) reveal that the heart and coronary vasculature plexus are grossly normal in *Smad4*$^{fl/fl}$ animals (*RosaCreER SMAD4*$^{fl/fl}$) at E13.5. (B-E) Quantification of heart size (control, *n*=5; *Smad4*$^{fl/fl}$, *n*=5) (B), coronary plexus migration onto the heart (control, *n*=5; *Smad4*$^{fl/fl}$, *n*=5) (C), number of intramyocardial capillary junctions (control, *n*=5; *Smad4*$^{fl/fl}$, *n*=5) (D), and intramyocardial capillary density (control, *n*=5; *Smad4*$^{fl/fl}$, *n*=5) (E) reveal that control and *RosaCreER Smad4* conditional knockout (CKO) (*Smad4*) mice are not significantly different. (F) Dilation of the coronary artery stem (dotted line) in *Smad4* CKO hearts occurs after connection with the aorta and establishment of blood flow. (G) Artery diameters at different embryonic stages in the indicated regions in controls (*n*=5-7), and mice with *Smad4* deletion induced by *RosaCreER* (*n*=5-12) and *ApjCreER* (*n*=6-8). Note that the diameter increases, spreading from the aortic connection point (stem) to more distal regions as time proceeds. (H) Confocal images of VE-cadherin (endothelial cells) and SM-MHC (artery smooth muscle) immunostaining reveal increased coronary artery size (arrowheads). Artery outlines are shown for comparison. (I,J) Quantification of SM-MHC^{+} smooth muscle in *RosaCreER Smad4* hearts at E15.5 (control, *n*=6; *Smad4*$^{fl/fl}$, *n*=6). (I) Coronary artery coverage. (J) Thickness of smooth muscle layer in the aorta. Data are mean±s.d. ns, non-significant; **P*≤0.05; ***P*≤0.01. CA, coronary artery. Scale bars: 100 µm in A; 50 µm in F; 100 µm in H.

reasons for the lack of cell alignment: (1) *SMAD4* is involved in the recognition of flow direction that is required to direct alignment; and (2) SMAD signaling specifically orchestrates the alignment response. To investigate these two possibilities, control and *SMAD4*-depleted HCAECs were stained for GOLPH4 (GOLIM4 – Human Gene Nomenclature Database), a Golgi marker, to indicate cell polarity (Franco et al., 2015). The results revealed that, even though there was no cell alignment, *SMAD4* knockdown cells were polarized against flow (Fig. 3A,C). Measuring the angle between the Golgi and nucleus revealed that *SMAD4* depletion causes a mild, but significant, decrease in polarization (Fig. 3D), which is in contrast to the dramatic effect on alignment (Fig. 3A). These data indicate that cell polarization in response to flow is either upstream or unrelated to the cell alignment response, and that only the latter is deeply dependent on SMAD signaling.

We next measured how cell area changed in control and *SMAD4*-depleted cells in response to flow. Cells were treated with either control or *SMAD4* siRNA for 24 h before plating in laminar flow chambers for 2 h, and cell areas were measured prior to or after the onset of flow. Cell areas were not significantly different before flow. However, exposure to shear stress decreased control cell areas but increased the size of *SMAD4* knockdown cells (Fig. 3E). These results showed that the size of *SMAD4*-deficient cells was not disrupted under normal conditions, but was abnormally increased in response to flow.

We next analyzed proliferation because an increase in cell number could lead to larger arteries. HCAECs depleted of *SMAD4* were exposed to shear stress via an orbital shaker and treated with 5-ethynyl-2′-deoxyuridine (EdU) for 3 h to label cycling cells. Cells were immunostained with VE-cadherin and DAPI and treated to reveal EdU incorporation. There was a significant decrease in proliferation when comparing control to *SMAD4*-depleted cells cultured under static, no-flow conditions (Fig. 3F). By contrast, *SMAD4*-depleted cells increased proliferation over controls when they were exposed to shear stress (Fig. 3F). Therefore, SMAD signaling functions as a restraint to shear stress-activated cell cycle progression *in vitro*.

SMAD4 is required for shear stress-directed cell migration

Because polarity was not dramatically affected by *SMAD4* deletion, we wondered whether flow-directed cell migration

Development (2017) 144, 3241-3252 doi:10.1242/dev.150904

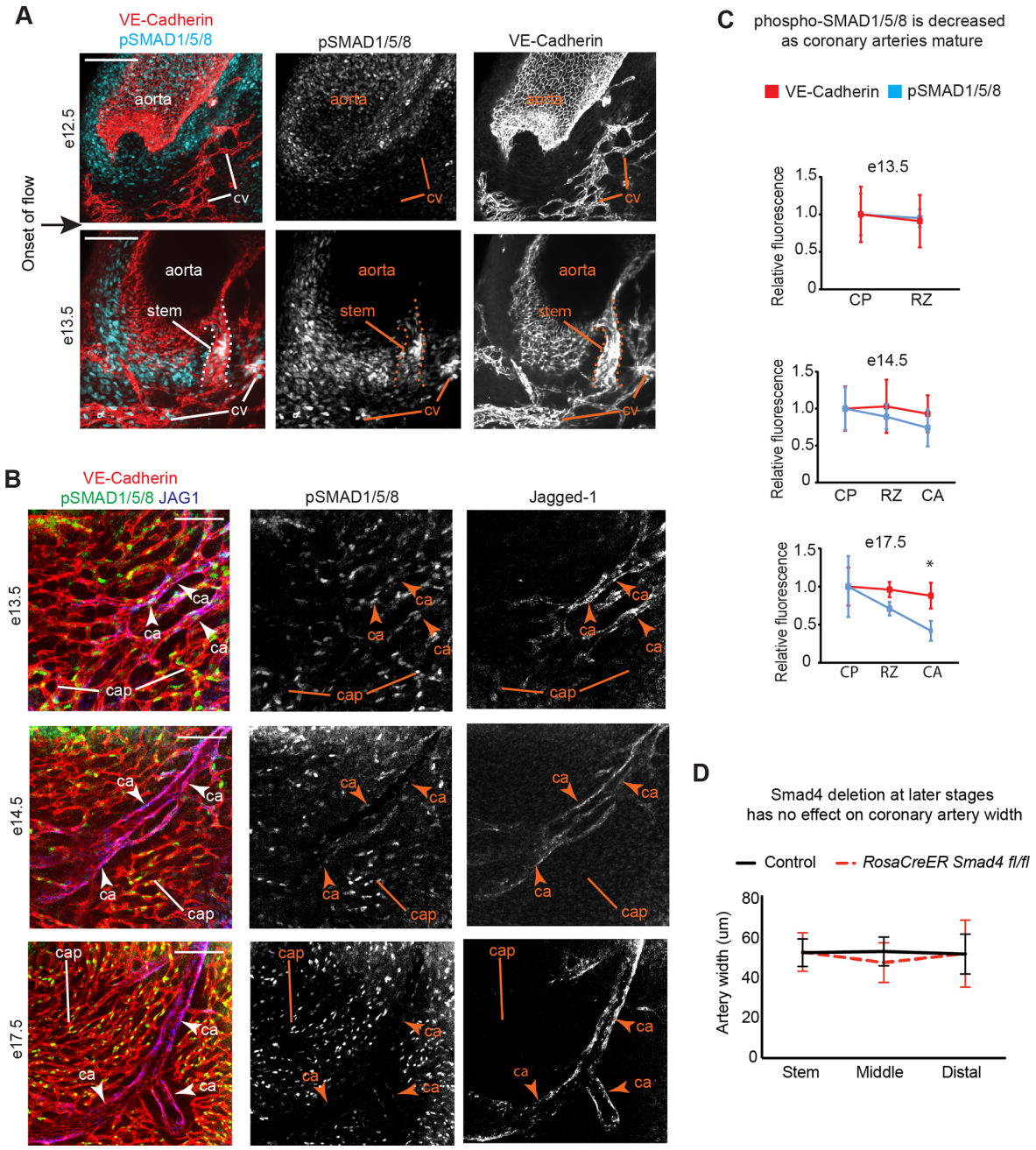

Fig. 2. SMAD1/5/8 is phosphorylated in coronary arteries following the onset of flow. (A) Confocal images of the coronary artery stem (dotted line) where it connects to the aorta, immunostained for pSMAD1/5/8, show activated protein in coronary vessels (stem and cv) following the onset of blood flow. (B) Images of the whole heart localizing jagged-1 with VE-cadherin and pSMAD1/5/8 at multiple developmental stages to label remodeling (high SMAD activation) and mature arteries (decreased SMAD activation). (C) Quantification of decreased pSMAD1/5/8 immunofluorescence at E17.5 when compared to VE-cadherin, which served as an internal control (wild type, n=6-12). (D) Deletion of *Smad4* using *RosaCreER* at E15.5-16.5 does not result in dilated arteries at E18.5 (control, n=7; *Smad4*$^{fl/fl}$, n=8). Data are mean±s.d. *$P \leq 0.05$. ca, coronary artery; cap, capillaries; cp, capillary plexus; cv, coronary vessels; rz, remodeling zone. Scale bars: 50 µm in A; 100 µm in B.

would also be intact despite the complete lack of cell alignment. Time-lapse images were taken of cells treated with control or *SMAD4* siRNA, and migration tracts were traced. Consistent with static data, control, but not mutant, cells aligned over time in culture (Fig. 4A and Movie 1). Alignment was not merely delayed because the *SMAD4*-deficient cells remained nonaligned at a 72 h time point (Fig. 4A and Movie 2). Tracing migration tracks throughout the culture period revealed that both cells were highly migratory (Movies 1 and 2). However, control cells mostly migrated against the direction of flow, while those lacking *SMAD4* moved randomly (Fig. 4B). Calculating average cell velocities showed that *SMAD4*-deficient cells moved at slightly higher velocities (Fig. 4C), but their rates along the axis of flow were dramatically lower than those of controls (Fig. 4D). The average total displacement of the cells against the direction of flow was also dramatically lower than that of controls (Fig. 4E). These differences were not caused by differences in cell density in these experiments (Fig. 4F). These data show that SMAD signaling is not required for migration, but

Development (2017) 144, 3241-3252 doi:10.1242/dev.150904

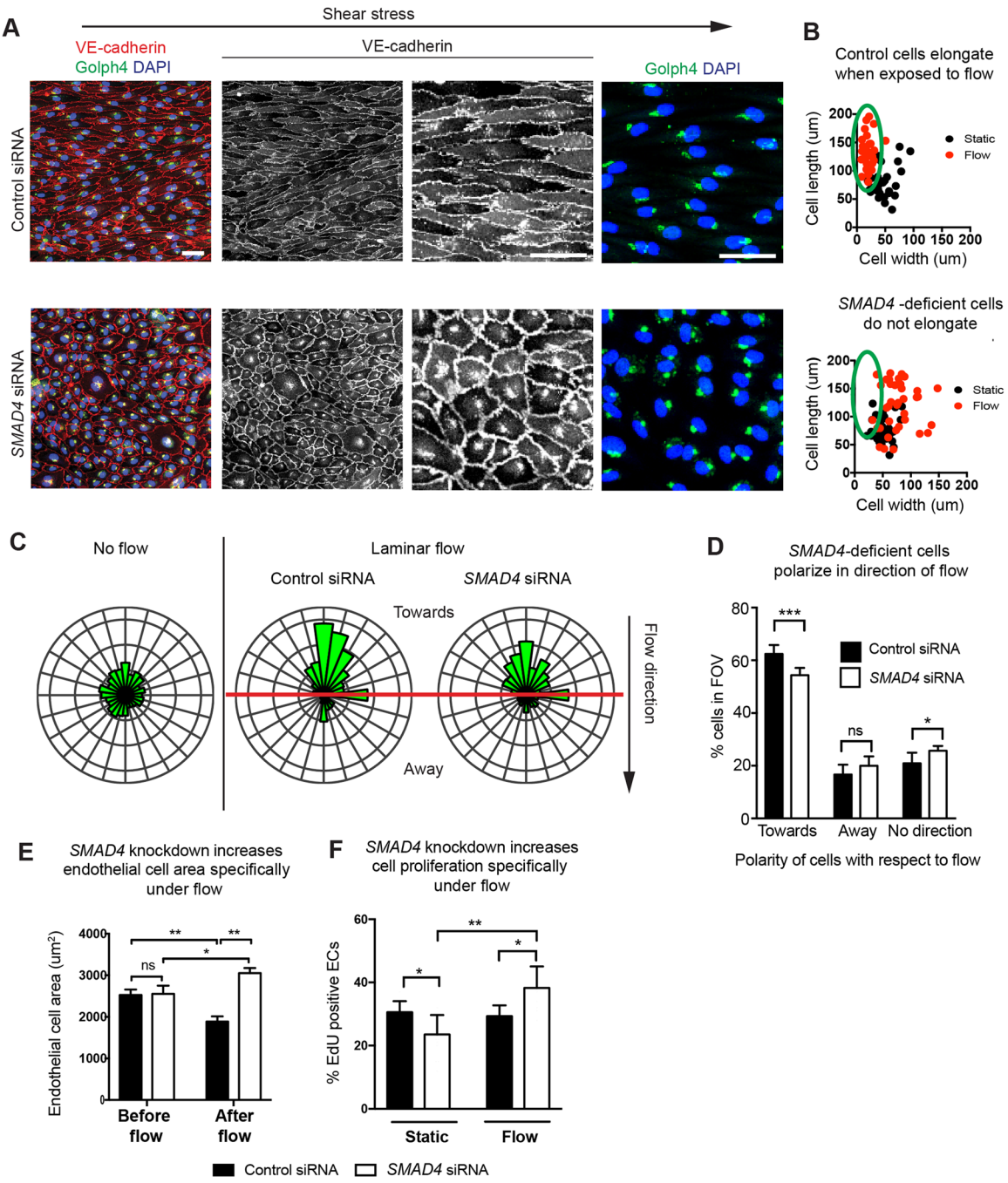

Fig. 3. *SMAD4* is required for endothelial cell alignment, but not polarization, along the axis of laminar fluid flow. (A) Human coronary endothelial cells exposed to shear stress in a laminar flow chamber do not align, but still polarize their Golgi (green, GOLPH4^{+}) against the direction of flow. VE-cadherin is shown in red; nuclei are labeled with DAPI (blue). (B) The absence of shear stress-induced alignment is quantified by plotting cell length versus width. Each dot is an individual cell. The green ovals indicate elongated cells. (C,D) Quantification of the angle between the nucleus, Golgi and flow showed a mild, but significant, decrease in polarization against flow. This is in contrast to the complete lack of alignment. Rose plots of measured angles are shown in C. *n*=140-300 cells per field of view. (E) Cell area is specifically increased under flow. (F) Quantification of proliferation rates through EdU incorporation. *Smad4* depletion results in increased proliferation under flow (orbital). Data are mean±s.d. ns, non-significant; **P*≤0.05; ***P*≤0.01; ****P*≤0.001. EC, endothelial cell; FOV, field of view. Scale bars: 20 µm.

rather for directing the migratory response against the direction of flow.

SMAD4 couples with other SMAD complexes to function as a transcription factor, suggesting that it could affect flow-directed behavior by inducing transcription of flow-sensitive or flow-responsive molecules. Thus, we used qPCR to investigate the expression levels of known flow sensors and *KLF2*, a flow responsive gene, in *SMAD4*-depleted cells. In contrast to the 80% decrease in *SMAD4* levels, the amounts of flow sensor *PECAM1*, VE-cadherin (*CDH5* – Human Gene Nomenclature Database), *VEGFR2* (*KDR*) and *PIEZO1* mRNA were unchanged (Fig. 4G). Furthermore, the increase in *KLF2* in the presence of shear stress was similar in control and knockdown cells (Fig. 4H). These observations indicate that SMAD signaling does not disrupt shear stress-mediated responses by

Development (2017) 144, 3241-3252 doi:10.1242/dev.150904

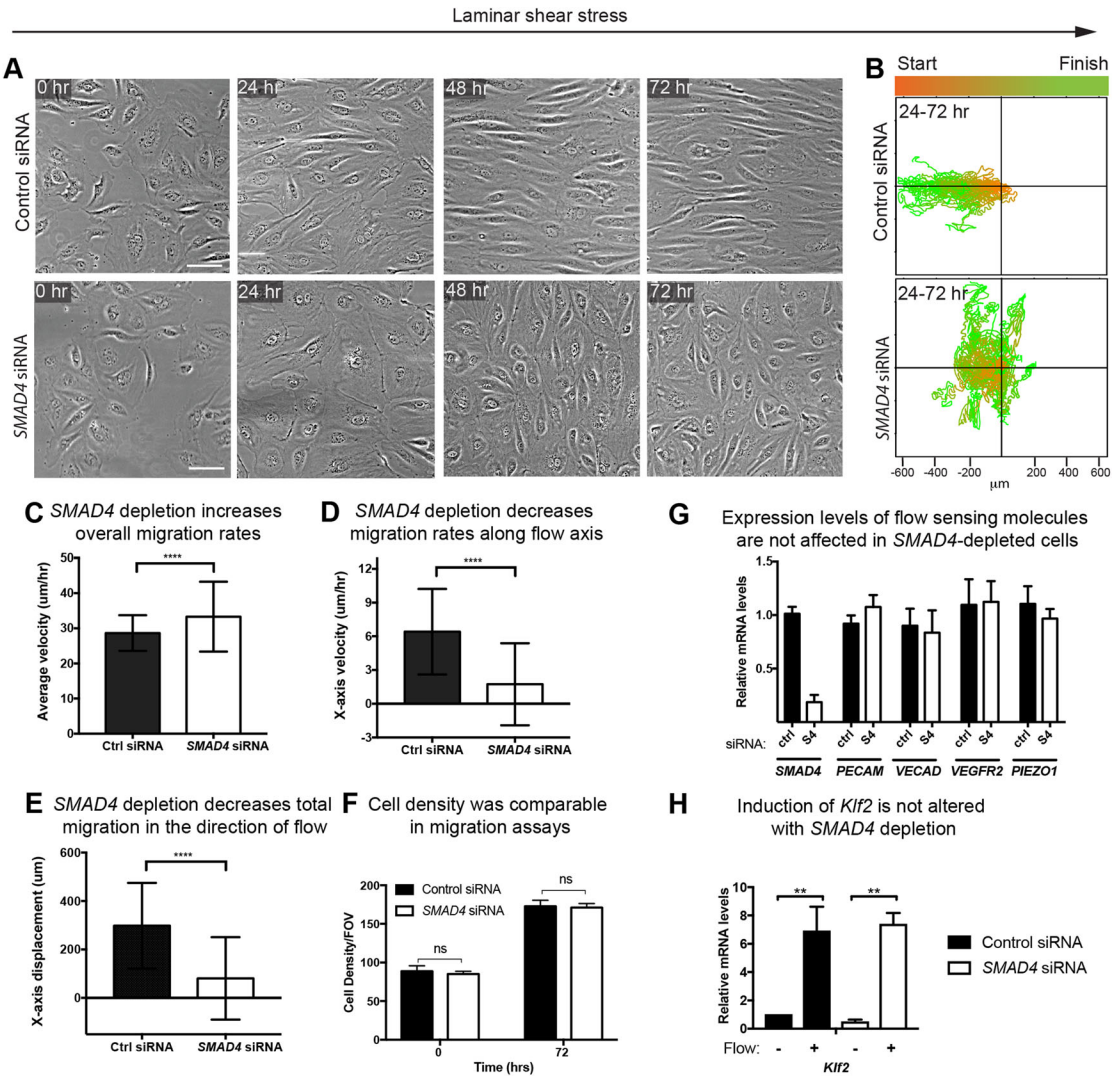

Fig. 4. Shear stress-guided cell migration is undirected in the absence of *SMAD4*. (A) Still micrographs from time-lapse imaging of control and *SMAD4* knockdown cells at the indicated times. (B) Plotting migratory tracts (30 cells shown) and color coding the start (orange) and end (green) points reveal that SMAD4-deficient cells migrate randomly instead of against the direction of laminar shear stress. (C-E) Quantification of >59 cells/condition showed a small, but significant, increase in general migration rates (C). By contrast, velocity (D) and total displacement (E) along the *x*-axis parallel to flow was almost completely diminished. (F) Cell density was the same across flow experiments. (G,H) Quantitative PCR for flow sensors (G) and flow responsive (H) genes. Data are mean±s.d. ns, non-significant; $^{**}P \leq 0.01$; $^{****}P \leq 0.0001$. Scale bars: 20 μm.

activating the transcription of the flow sensors assayed here, or by inhibiting *KLF2* induction.

SMAD4 deficiency increases arterial cell size and proliferation *in vivo*

Because *SMAD4* depletion in cell culture resulted in nonaligned cells that increased proliferation in response to flow, we assessed whether this also occurred in coronary arteries *in vivo*. We found that arterial endothelial cells aligned parallel to flow; however, their cell size was much larger, similar to those after *in vitro* knockdown (Fig. 5A). Measuring the length and width of the cells (Fig. 5B) and total cell area (Fig. 5C) revealed significant increases in cell size. Interestingly, this increase in vessel diameter and cell size was accompanied by a decrease in the width of the avascular zone that surrounds most arteries (Fig. 5A,D). Therefore, as *in vitro*, SMAD signaling restrains endothelial cell size in developing coronary arteries.

We next investigated whether the increases in artery diameter could be fully accounted for by the increases in cell width. The relative increase in mutant diameters over controls was compared to the relative increase in the width of individual mutant cells over controls. These results showed that mutant arteries were, on average, 81% wider than controls, while individual mutant cells were, on average, 41% wider than controls (Fig. 5E). These data indicate that increased cell width *in vivo* cannot fully account for the larger artery phenotype.

To investigate another parameter that could lead to increased diameter, proliferation of arterial endothelial cells was also assessed. E15.5 dams harboring either control or *Smad4* conditional knockout embryos were treated with EdU before hearts were collected, immunostained and analyzed for EdU incorporation. Even in the early stages of their development, arterial endothelial cells in the developing heart very rarely proliferate, and this was also true in control hearts (Fig. 5F). By contrast, coronary arteries from *Smad4* conditional knockout animals contained a higher number of EdU^{+} (cycling) endothelial cells (Fig. 5F,G). This was accompanied by an increase in cell

Development (2017) 144, 3241-3252 doi:10.1242/dev.150904

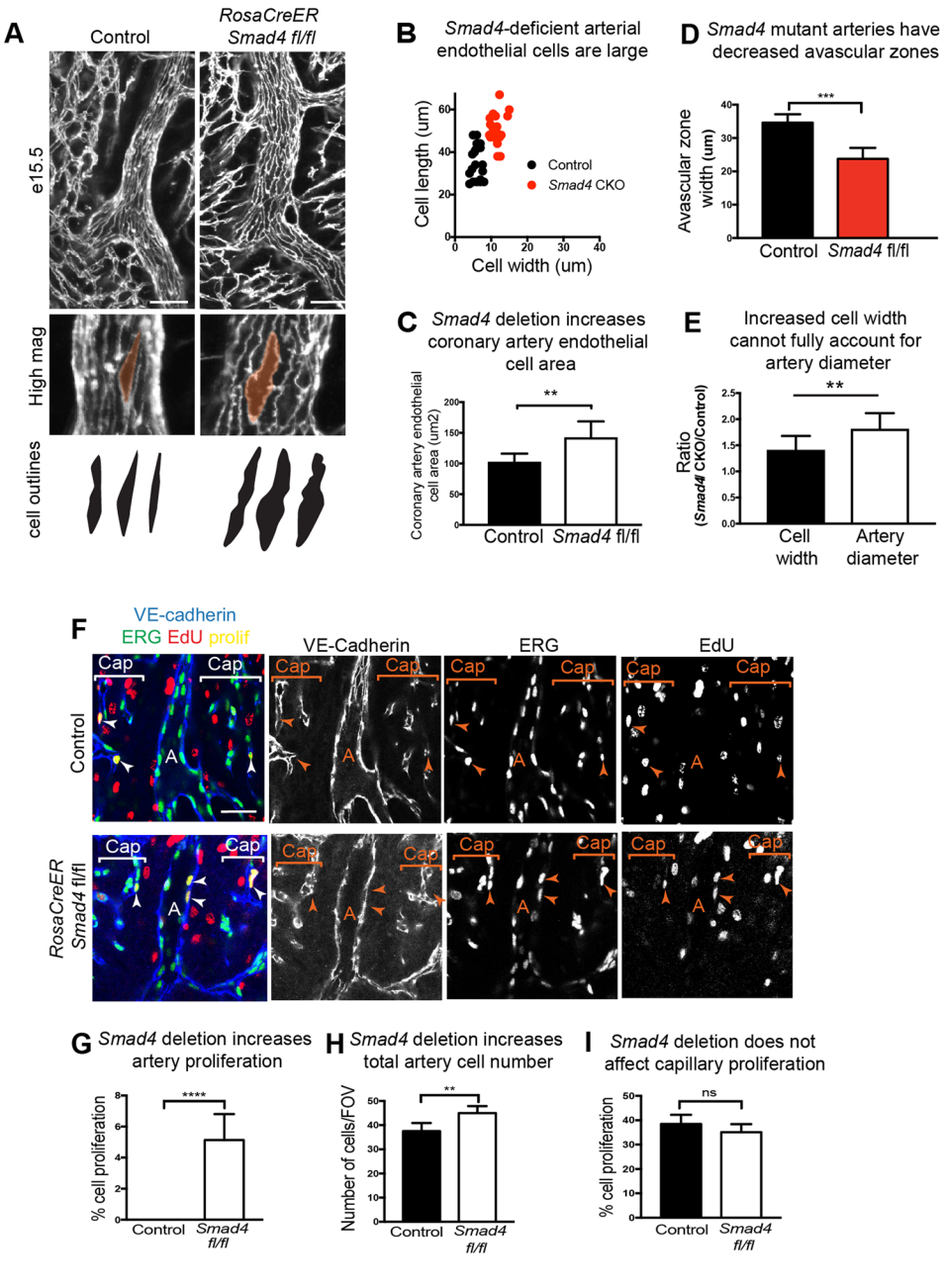

Fig. 5. Cell alignment and proliferation are perturbed in *Smad4*-depleted arteries. (A,B) Decreased cell shape changes and alignment *in vivo* in *RosaCreER Smad4*$^{fl/fl}$ coronary arteries at E15.5. (A) Confocal immunofluorescent images of VE-cadherin immunostaining. (B) Cell size measurements; each dot represents a single cell. (C) Quantification of cell area (control, *n*=6; *RosaCreER Smad4*$^{fl/fl}$, *n*=7). (D) Measurement of avascular zones, (control, *n*=6; *Smad4* CKO, *n*=7). (E) Relative increase in individual cell width and vessel diameters (control, *n*=5; *RosaCreER Smad4*$^{fl/fl}$, *n*=6). (F) *In vivo* EdU incorporation to assess cell proliferation identifies EdU/Erg double-positive endothelial nuclei only in mutant arteries at E15.5. (G-I) Quantification shows that *Smad4* deletion significantly increases artery proliferation (control, *n*=5; *RosaCreER Smad4*$^{fl/fl}$, *n*=6) (G) and cell numbers (control, *n*=5; *RosaCreER Smad4*$^{fl/fl}$, *n*=6) (H), but does not affect capillary proliferation (control, *n*=5; *RosaCreER Smad4*$^{fl/fl}$, *n*=6). Data are mean±s.d. ns, non-significant; $^{**}P \leq 0.01$, $^{****}P \leq 0.0001$. A, artery; Cap, capillaries. Scale bars: 50 µm.

number within the artery wall (Fig. 5H). Similar to the structural measurement of capillary vessels shown in Fig. 1, there was no difference in capillary proliferation rates between control and *Smad4* conditional hearts (Fig. 5I). These data show that SMAD4 suppresses cell proliferation and increases cell number specifically in arterial vessels.

BMP inhibition through noggin phenocopies the lack of alignment with *Smad4* siRNA

Since SMAD4 propagates signals from many different TGFβ superfamily ligands and can be activated by shear stress in a ligand-independent manner (Zhou et al., 2012), we next aimed to test candidate factors upstream of the alignment response. The expression pattern of pSMAD1/5/8, which is downstream of BMP signaling, suggested that BMP ligands could stimulate SMAD4 in coronary arteries (Fig. 2). Noggin (NOG) is a naturally occurring, secreted broad spectrum BMP inhibitor that blocks signaling via BMP2/4/5/7/13/14 (Krause et al., 2011). A NOG-Fc fusion protein was added to HCAECs that were exposed to orbital flow for 24 h, and cell alignment was assessed. Control cells treated with an irrelevant Fc fusion protein (CD6-Fc) aligned parallel with the direction of flow. However, NOG-Fc-treated cells resembled those subjected to *SMAD4* knockdown in that they failed to align (Fig. 6A,B). Also, similar to *SMAD4* knockdown conditions, they retained polarization against the direction of flow as assessed by Golgi positioning (Fig. 6C). Total cell area was also increased specifically under flow (Fig. 6D). These data show that BMP ligands mediate SMAD signaling to activate cell alignment in cultured HCAECs.

DISCUSSION

Here, we show that SMAD4 is critical for restraining coronary artery size during embryonic development, and provide evidence that it functions through regulating shear stress-guided cell shape changes,

Development (2017) 144, 3241-3252 doi:10.1242/dev.150904

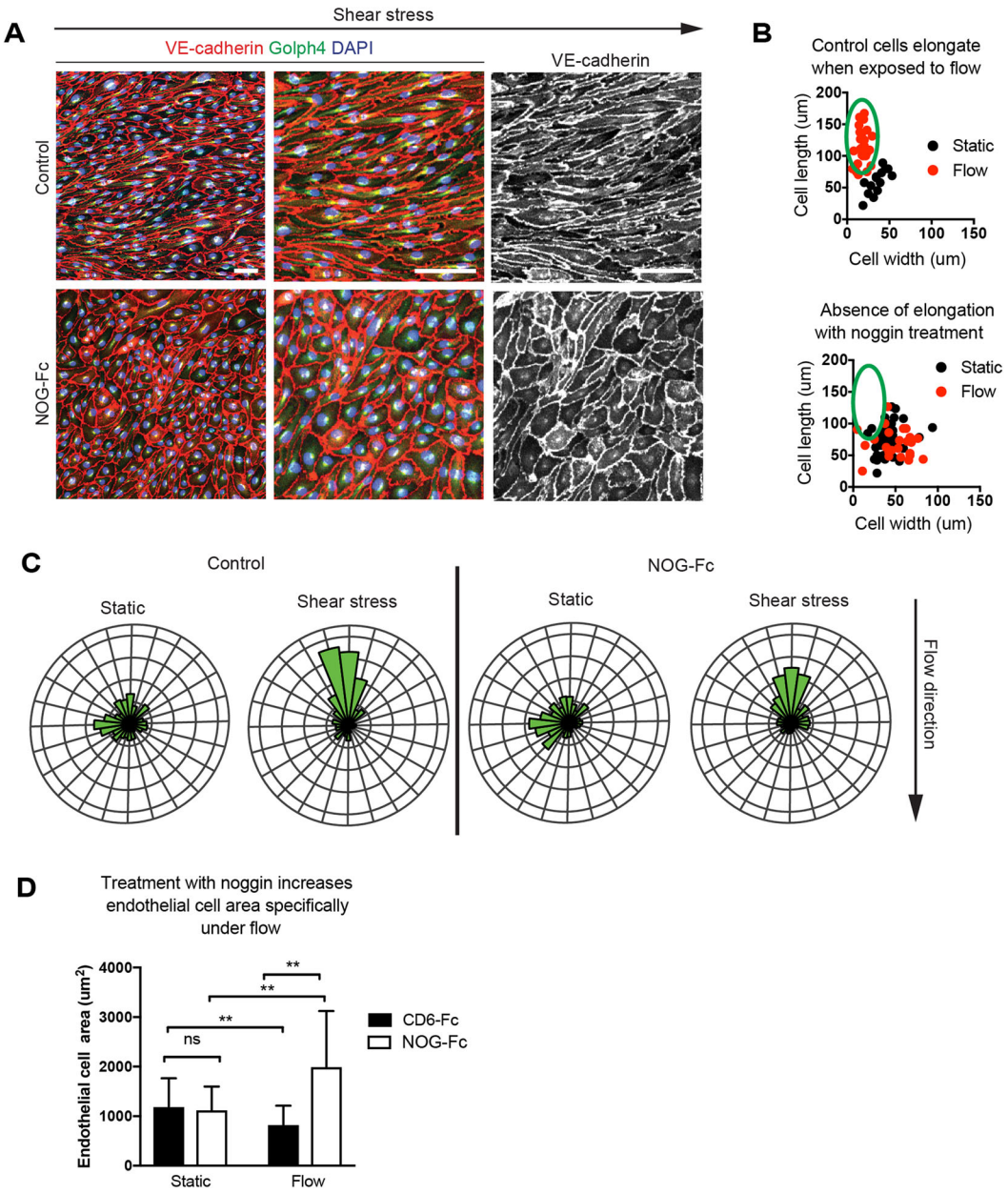

Fig. 6. BMP inhibition phenocopies *Smad4*-depleted cells. (A) HCAECs were treated with a BMP inhibitor (NOG-Fc) or control protein (CD6-Fc) and exposed to laminar shear stress through orbital rotation. Immunofluorescence for the indicated proteins highlights the absence of alignment specifically in the presence of NOG-Fc. (B) Quantification of alignment (cell width versus length). Each cell is represented by a dot, and the green ovals indicate elongated cells. (C) Rose plots show that cells remain aligned with BMP inhibition. (D) Cell area is specifically increased under flow. *n*=140-300 cells per field of view. Data are mean±s.d. ns, non-significant; $^{**}P \leq 0.01$. Scale bars: 50 µm in the middle and right-hand panels in A; 100 µm in the left-hand panel in A.

migration, and proliferation. Conditional deletion of *Smad4*, either ubiquitously or in sinus venosus-derived coronary endothelial cells, resulted in an increase in arterial vessel diameter coincident with the onset of blood flow. The phenotype also temporally correlated with increased SMAD1/5/8 activation. Because the defects in coronary arteries and the high levels of phosphorylated SMAD1/5/8 were only seen after blood flow was present, we hypothesized that SMAD signaling might be mediating flow-induced responses. Indeed, either *SMAD4* depletion or BMP inhibition in coronary artery endothelial cells completely blocked their ability to align parallel to flow. Although general migration was not inhibited, the ability of cells to move against the direction of flow was blocked in the absence of SMAD4, suggesting that it is required specifically for perceiving flow direction or for carrying our directed migration in response to another direction sensor. In contrast to the effects on alignment and directed migration, cell polarization against the direction of flow (as assessed by Golgi localization) was still intact, showing that sensing flow direction to provide polarization is either upstream or separate from alignment and migration. *SMAD4* knockdown cells also displayed increased proliferation, specifically in the presence of flow. These alterations in flow-induced endothelial cell behaviors likely contributed to increased coronary artery size in conditional mutants, which showed decreased alignment and increased endothelial proliferation. Thus, SMAD signaling regulates specific modules of the flow response in endothelial cells to affect artery size.

Development (2017) 144, 3241-3252 doi:10.1242/dev.150904

How endothelial cells sense and respond to small fluctuations in shear stress is fascinating cell biology, but also holds implications for human disease. Mutations in *ALK1*, *ENG* and *SMAD4* are found in the majority of patients suffering from HHT, a heritable genetic disorder characterized by abnormal blood vessel structures, including telangiectasias and AVMs (McDonald et al., 2015). These abnormalities are highly susceptible to rupture, and are thought to arise during vascular development. In zebrafish and mice, loss of *Alk1* or *Eng*, either embryonically or in the adult, leads to HHT-like hemorrhages and the development of AVMs (Sorensen et al., 2003; Baeyens et al., 2016b; Jin et al., 2017; Sugden et al., 2017; Tual-Chalot et al., 2015). Understanding the underlying cellular defects leading to HHT is thus an important goal in vascular biology.

Evidence indicates that BMP/SMAD signaling normally suppresses telangiectasias and AVMs through activating vascular quiescence in response to blood flow. Laminar shear stress is known to stimulate vascular quiescence (Roman and Pekkan, 2012). In zebrafish, *alk1* expression in arteries is induced by shear stress, where the receptor subsequently binds circulating BMP10 to limit artery size and AVMs (Corti et al., 2011; Laux et al., 2013). As a result, deleting/depleting *alk1* or *bmp10* results in supernumerary endothelial cells, increased arterial caliber, and persistent AVMs (Laux et al., 2013). In mice, BMP/SMAD signaling controls the angiogenic response. Blocking circulating BMP9 and BMP10 dramatically increases retinal angiogenesis, producing a hypervascularized postnatal retina with increased vessel caliber and loss of arterial gene expression (Larrivée et al., 2012; Moya et al., 2012). A similar phenotype is obtained upon inhibition of Notch, and further analyses showed that BMP9/10 activation of Alk1 functions by potentiating Notch signaling (Larrivée et al., 2012; Moya et al., 2012). BMP/SMAD signaling is also required throughout life to maintain vascular integrity. Deletion of *Alk1* in the adult causes highly dilated vessels, hemorrhages, and AVMs (Park et al., 2009). Flow potentiates BMP/SMAD signaling using the Eng co-receptor, which could explain why AVMs in Alk1 mutants develop specifically in the presence of high flow (Baeyens et al., 2016b). Thus, BMP/SMAD signaling appears to be critical for regulating vascular growth stimulated by high flow to produce and maintain stabilized blood vessels, a function that goes awry in HHT.

BMP/SMAD signaling is emerging as an important mediator of how endothelial cells respond to flow, which in turn shapes vascular structure. In zebrafish, the increasing flow strength that occurs during embryonic development activates endothelial cell shape changes that contract the aorta, a response that does not occur in *eng* mutants (Sugden et al., 2017). Our data that SMAD1/5/8 is activated for a limited time window following the onset of blood flow, and that deleting *Smad4* after this window does not affect the size of the main coronary artery stem, suggests a similar response in the mammalian heart. Specifically, there may be an initial response to increasing shear stress that triggers cell size decreases that restrain artery size. SMAD-stimulated migration also contributes to vascular structure. Endothelial cells migrate against flow into arteries (Franco et al., 2016; Sato et al., 2010; Udan et al., 2013; Xu et al., 2014), and this is inhibited in *Eng*-deficient mice (Jin et al., 2017). As is seen in *alk1* zebrafish mutants (Rochon et al., 2016), the inability of *Smad4*-deficient coronary endothelial cells to migrate against the direction of flow could lead to an abnormal accumulation of cells within the arteries. This, along with increased cell proliferation, could expand artery size. Further studies on SMAD-regulated endothelial cell biology could increase our knowledge on flow-guided vessel growth and homeostasis.

We provide evidence that BMPs are the ligands for SMAD4-guided cell shape changes in response to flow. Adding NOG-Fc, which inhibits a number of BMPs, to our orbital cultures abrogated shear stress-induced alignment. How a secreted ligand could provide spatial information in our cell culture remains an open question. It could involve asymmetrically tethering of the ligand to the cell surface. Alternatively, SMAD signaling could be required to render the cells permissive to another spatially asymmetrical signal. BMP4 is a candidate for mediating SMAD4 signaling *in vivo*. Expression databases (e.g. Genepaint and Allan Brain Atlas) show that BMP4 is highly expressed in aortic endothelium. Coronary attachment to the aorta (the event that directly precedes the *Smad4* phenotype) could initiate access to BMP4 flowing downstream into coronary arteries. However, how BMPs translate directional information *in vitro*, and whether BMPs or a TGFβ-activated response (or both) are involved in the *in vivo* phenotype, awaits future investigation.

Future experiments will also investigate the downstream interactions that cause SMAD to influence the cytoskeletal/cell migration machinery in an asymmetric manner. Because SMADs are transcription factors, a likely scenario is that they activate the expression of molecules that sense and respond to flow. Several classes of molecules are also required for the alignment response. Shear stress-induced integrin binding activates Rho and Rac GTPases, leading to changes in the cytoskeleton and alignment, as well as gene expression changes (Collins and Tzima, 2014; Tzima et al., 2002). Flow creates changes in tension on a VEGFR2/PECAM1/VE-cadherin complex that activate Src family kinase signaling and induce cell alignment (Chiu et al., 2008; Collins et al., 2012; Conway et al., 2013; Tzima et al., 2005). Flow can also activate the mechnosensitive ion channel PIEZO1 to stimulate cell alignment (Li et al., 2014; Ranade et al., 2014). Cells lacking the transmembrane heparan sulfate proteoglycan syndecan 4 do not align or properly activate transcription under flow (Baeyens et al., 2014). These factors also mediate endothelial cell alignment within the vessel (Baeyens et al., 2014; Li et al., 2014; Tzima et al., 2005). Initial investigations excluded the hypothesis that SMADs function by activating the transcription of the VEGFR2/PECAM1/VE-cadherin complex or *PIEZO1*. However, a broader analysis could identify other known or novel flow sensors downstream of SMAD4. It will also be interesting to examine how SMAD signaling relates to pathways controlled by the apelin receptor, APJ (APNLR), which mediates shear stress-induced cell polarity (Wang et al., 2016). Understanding how SMAD-mediated transcription is required for shear stress-directed cell biology will shed light on how endothelial cells integrate this environmental cue to shape the vasculature.

MATERIALS AND METHODS

Animals

The Institutional Animal Care and Committee (IACUC) at Stanford University approved all experiments and protocols performed on mice for this study. Male and female *Smad4* conditional mice (aged 6-8 weeks) were maintained on a C57BL/6 background as previously described (Chu et al., 2004). Male and female CD1 mice (aged 6-8 weeks) were obtained from Charles River (strain code 022). CD1 mice were used for pSMAD1/5/8 expression.

Immunofluorescence and imaging

Different staged embryonic hearts were obtained, dissected and fixed in 4% paraformaldehyde, and then washed and stored at 4°C in PBS. Whole mount fluorescence microscopy was performed on intact hearts immunostained with the following protocol. Primary antibodies were diluted in blocking solution and 5% goat serum with 0.5% Triton X-100, and incubated overnight at 4°C. Then, hearts were washed with PBT (PBS with 0.5%

Development (2017) 144, 3241-3252 doi:10.1242/dev.150904

Triton X-100) four times for 1 h and incubated with diluted secondary antibodies in blocking solution overnight. Tissues were then washed again at room temperature, placed in Vectashield (Vector Laboratories, H-1000), and imaged using an inverted Zeiss LSM-700 confocal microscope. Embryonic hearts were oriented in an eight-well-chambered coverslip to invariably image the coronary arteries and other surrounding vasculature. All images were digitally captured and processed using Zeiss Zen software (2011 version).

Antibodies

VE-cadherin (BD Biosciences; 550548, 1:100 and 555661, 1:500), SM-MHC (Biomedical Technologies, BT-562, 1:300), GOLPH4 (Abcam, ab28049, 1:1000), cTNT (Developmental Studies Hybridoma Bank, CT3-c, 1:500), JAGGED-1 (R&D Systems, AF599, 1:125), ERG (Abcam, ab92513, 1:500) and pSMAD1/5/8 (rabbit anti-pSmad1/5/8, 1:1000; provided by Ed Laufer, Columbia University, New York, USA) primary antibodies were used. Secondary reagents were Alexa Fluor 488-, 555- and 637-conjugated antibodies (Life Technologies, 1:250). DAPI was obtained from Sigma-Aldrich (D9542) and used at 2 µg/ml. For western blot analysis, SMAD4 (Abcam, ab40759, 1:2000) and α-tubulin (Santa Cruz Biotechnology, sc-530300, 1:2000) were used.

Measurement of coronary artery and vein size, and vessel structural parameters

Endothelial cells of embryonic hearts (E12.5, E13.5, E14.5, E15.5 and E18.5) were labeled with VE-cadherin and imaged using whole mount confocal microscopy. Heart size and coronary vessel migration were measured in E14.5 hearts using ImageJ software. The freeform selection tool was used to circumscribe the whole dorsal side of the heart (heart size) and the area covered by coronary vasculature (coronary coverage). The number of capillary junctions, vessel density and vessel length were measured using Angiotool software as described previously (Zudaire et al., 2011). The artery and vein diameters were measured at three different locations along the length of the coronary artery: stem/proximal, middle and distal area (n=5-12). Values were averaged from the controls (Cre^+, $flox^+$ or Cre^- flox/flox) or experimental mice (Cre^+ flox/flox). The widths of the avascular region around the coronary arteries, aortic lumen, sinotubular junction, and right and left leaflets were measured in control or experimental mice using Zeiss Zen software.

Quantification of smooth muscle fluorescence

The smooth muscle of the developing coronary artery and the aorta were immunolabeled with SM-MHC. To quantify the area covered by the smooth muscle cells, a length of ∼400 µm from E15.5 hearts was cropped from a maximal projection excluding the surface optical planes from the right coronary artery. The cropped area was then quantified to determine the total area of the artery. The same threshold parameter was then applied to the SM-MHC-labeled channel to quantify the area covered by the smooth muscle. The percentage coverage was calculated by dividing the total area by the area covered with smooth muscle. For the aorta, the thickness of smooth muscle was quantified using optical sections from the z-stacks of confocal images (n=5-6 hearts per group).

Quantification of pSMAD1/5/8 fluorescence

pSMAD1/5/8 expression levels of E12.5, E13.5, E14.5 and E17.5 embryos were quantified from confocal images of the hearts, immunostained for VE-cadherin and pSMAD1/5/8. Expression in the capillary plexus, remodeling zone, and coronary arteries were quantified from the same z-plane by selecting a line segment along the endothelial cells of each heart in ImageJ. Then, average fluorescence intensity was calculated for each segment (n=5-8 hearts per time point). VE-cadherin served as a control.

qPCR analysis

RNA was isolated with an RNeasy Plus Mini Kit (Qiagen, 74104), and 100 ng was used for the RT reaction using iScript RT mix (Bio-Rad, 1708840). qPCR was performed using iTaq Universal Sybr Green Supermix (Bio-Rad, 1725121) and run on a CFX96 Touch Real-Time PCR Detection System (Bio-Rad). Primers were designed and ordered from Integrated DNA Technologies using the PrimerQuest Real-Time PCR Design tool. Primers for the following genes were designed: *SMAD4*, *VEGFR2*, VE-cadherin, *PIEZO1* and *KLF2*. *GADPH* served as a control.

Proliferation in endothelial cells (*in vitro*)

Depletion of SMAD4 in primary endothelial cell cultures was achieved through siRNAs purchased from Sigma-Aldrich (human SMAD4) and scramble siRNA served as control. HCAECs were transfected using RNAiMax (Invitrogen) with 10 pmol siRNA per six-well plate according to the manufacturer's instructions and used for 24 h. Cells were subjected to two types of fluid shear stress: parallel plate and orbital shaker. Cells plated for orbital shaker experiments were incubated for 24 h to allow EdU incorporation. Subsequently, cells were fixed with 4% paraformaldehyde and EdU incorporation was detected using a Click-iT EdU Alexa Fluor 555 Imaging Kit (Thermo Fisher Scientific, C10338) as per the manufacturer's protocol. Cell nuclei were co-stained with DAPI (1:500). For quantification, five fields per well were photographed at 10× magnification and proliferation rates were calculated as a ratio of EdU^+ cells per total number of cells stained with DAPI. Cells were counted using the ImageJ cell counter tool.

Exposure of endothelial cells to shear stress

Orbital shaker

HCAECs were plated in six-well plates at 70-80% confluency, placed on an orbital shaker to generate laminar shear stress and cultured for 24 h. The orbital shaker was set at 210 rpm to recapitulate a shear stress of ∼14 dyne/cm^2 (Dardik et al., 2005). After 24 h, the cells were collected for qPCR experiments or immunostaining as shown in Figs 3 and 6. For *SMAD4* knockdown, siRNA (Sigma-Aldrich, EHU018671) was applied 24 h prior to rotation. For BMP inhibitor experiments, either NOG-Fc (300 ng/µl, R&D Systems) or CD6 (300 ng/µl, R&D Systems) was added at the initiation of rotation. All experiments were repeated in triplicate.

Parallel plate chamber

HCAECs were plated at 70-80% confluency in each lane of a µ-Slide $VI^{0.4}$ (ibidi, 80601) coated with fibronectin (Sigma-Aldrich, F0895, 1:100) 2 h prior to the experiment. The culture medium consisted of Leibowitz's L-15 medium without Phenol Red (Thermo Fisher Scientific, 21083-027) supplemented with EGM2-MV SingleQuot Kit Supplement and Growth Factors (Lonza, CC-4147). Uniform laminar shear stress at 35 dynes/cm^2 was generated by attaching slide chambers to a pump system (ibidi, 10902) mounted on an inverted microscope (Zeiss Axio Observer Z1) fitted with a heated Plexiglass enclosed incubator. Time-lapse images were taken every 15 min, starting 30 min after pump initiation. Cell migration tracts were analyzed using the mTrackJ plug-in provided by Fiji software for tracking an individual cell from the time-lapse images taken under flow conditions (described above). A total of 30 randomly selected cells from three fields of view were quantified from each of three experiments (total of 90 cells per condition). For *SMAD4* knockdown, siRNA (Sigma-Aldrich, EHU018671) was applied 24 h prior to plating and flow initiation.

Cell polarization

To measure cell polarization, HCAECs were stained for the Golgi (GOLPH4) and nuclei (DAPI). Fluorescent images were processed in ImageJ using the straight line tool. The location of the nucleus and Golgi of each cell were quantified. For each cell, two points were noted; the first being the center of the nucleus and the second being the center of the Golgi, which defined an angle between the two points relative to the direction of flow. A total of three fields of view from each experiment were quantified per condition.

Measurement of coronary artery endothelial cell shape, size and alignment

Cell shape and alignment were measured in coronary arteries of mouse embryonic hearts in controls and *Smad4* conditional knockouts at E15.5. To measure cell shape in coronary arteries, hearts were stained for VE-cadherin

Development (2017) 144, 3241-3252 doi:10.1242/dev.150904

to label endothelial cell borders. Cell shape and alignment was determined by measuring individual arterial endothelial cell length and width using Zeiss Zen software (version 2011).

In vivo proliferation

Cell proliferation was measured via the incorporation of EdU to assess the mitotically active cells in mouse hearts. Pregnant females received a single intraperitoneal injection of 400 µg EdU dissolved in 200 µl dimethyl sulfoxide (DMSO). After 3 h embryonic hearts were dissected, fixed, and immunostained for VE-cadherin and Erg1. Subsequently, EdU incorporation into DNA was detected using a Click-iT EdU Alexa Fluor 555 Imaging Kit (Life Technologies, C10338), according to the manufacturer's protocol. Confocal *z*-stacks at 20× magnification through the right lateral side of each heart were obtained. A 300×300 µm square was drawn around the vascular plexus and developing coronary artery. All Erg^+ cells were counted using the cell counter plug-in of ImageJ. The percentage of those also positive for EdU was considered as proliferative. Fields of view were collected and analyzed from both control and mutant genotypes (n=4-6) at E14.5. Total arterial cell number was counted along 500 µm lengths of the developing artery using ImageJ software.

Statistics

Statistical analyses were performed using Prism (GraphPad). Data are mean±s.d. Unpaired *t*-tests (two-tailed) or Mann–Whitney U tests were performed to assess the statistical significance of differences between the groups. $P<0.05$ was considered statistically significant.

Acknowledgements

We thank Dr Elizabeth J. Robertson for providing the *Smad4* conditional knockout mouse line; and Drs Ed Laufer, Dan Vasiliauskas, Susan Morton and Thomas Jessell for providing pSMAD1/5/8 antibodies, which they generated collaboratively in their laboratories at Columbia University, New York, USA.

Competing interests

The authors declare no competing or financial interests.

Author contributions

Conceptualization: K.R.-H.; Methodology: A.P., B.R., S.R., M.V.; Software: A.P., A.H.C.; Validation: A.P., B.R., A.H.C.; Formal analysis: A.P., B.R., A.H.C., M.V., K.R.-H.; Investigation: A.P., K.R.-H.; Resources: K.R.-H.; Data curation: A.P.; Writing - original draft: A.P., K.R.-H.; Writing - review & editing: A.P., K.R.-H.; Visualization: K.R.-H.; Supervision: K.R.-H.; Project administration: K.R.-H.; Funding acquisition: K.R.-H.

Funding

This study was supported by the Office of Extramural Research, National Institutes of Health (R01HL128503 to K.R.-H.), the American Heart Association (AHA15PRE23020030 to A.H.C.) and the New York Stem Cell Foundation (Robertson Investigator to K.R.-H.). Deposited in PMC for release after 12 months.

Supplementary information

Supplementary information available online at
http://dev.biologists.org/lookup/doi/10.1242/dev.150904.supplemental

References

Baeyens, N., Mulligan-Kehoe, M. J., Corti, F., Simon, D. D., Ross, T. D., Rhodes, J. M., Wang, T. Z., Mejean, C. O., Simons, M., Humphrey, J. et al. (2014). Syndecan 4 is required for endothelial alignment in flow and atheroprotective signaling. *Proc. Natl. Acad. Sci. USA* **111**, 17308-17313.

Baeyens, N., Bandyopadhyay, C., Coon, B. G., Yun, S. and Schwartz, M. A. (2016a). Endothelial fluid shear stress sensing in vascular health and disease. *J. Clin. Invest.* **126**, 821-828.

Baeyens, N., Larrivée, B., Ola, R., Hayward-Piatkowskyi, B., Dubrac, A., Huang, B., Ross, T. D., Coon, B. G., Min, E., Tsarfati, M. et al. (2016b). Defective fluid shear stress mechanotransduction mediates hereditary hemorrhagic telangiectasia. *J. Cell Biol.* **214**, 807-816.

Chen, H. I., Sharma, B., Akerberg, B. N., Numi, H. J., Kivelä, R., Saharinen, P., Aghajanian, H., McKay, A. S., Bogard, P. E., Chang, A. H. et al. (2014). The sinus venosus contributes to coronary vasculature through VEGFC-stimulated angiogenesis. *Development* **141**, 4500-4512.

Chiu, J.-J. and Chien, S. (2011). Effects of disturbed flow on vascular endothelium: pathophysiological basis and clinical perspectives. *Physiol. Rev.* **91**, 327-387.

Chiu, Y.-J., McBeath, E. and Fujiwara, K. (2008). Mechanotransduction in an extracted cell model: Fyn drives stretch- and flow-elicited PECAM-1 phosphorylation. *J. Cell Biol.* **182**, 753-763.

Chu, G. C., Dunn, N. R., Anderson, D. C., Oxburgh, L. and Robertson, E. J. (2004). Differential requirements for Smad4 in TGFbeta-dependent patterning of the early mouse embryo. *Development* **131**, 3501-3512.

Collins, C. and Tzima, E. (2014). Rac[e] to the pole: setting up polarity in endothelial cells. *Small GTPases* **5**, e28650.

Collins, C., Guilluy, C., Welch, C., O'Brien, E. T., Hahn, K., Superfine, R., Burridge, K. and Tzima, E. (2012). Localized tensional forces on PECAM-1 elicit a global mechanotransduction response via the integrin-RhoA pathway. *Curr. Biol.* **22**, 2087-2094.

Conway, D. E., Breckenridge, M. T., Hinde, E., Gratton, E., Chen, C. S. and Schwartz, M. A. (2013). Fluid shear stress on endothelial cells modulates mechanical tension across VE-cadherin and PECAM-1. *Curr. Biol.* **23**, 1024-1030.

Corti, P., Young, S., Chen, C.-Y., Patrick, M. J., Rochon, E. R., Pekkan, K. and Roman, B. L. (2011). Interaction between alk1 and blood flow in the development of arteriovenous malformations. *Development* **138**, 1573-1582.

Culver, J. C. and Dickinson, M. E. (2010). The effects of hemodynamic force on embryonic development. *Microcirculation* **17**, 164-178.

Dardik, A., Chen, L., Frattini, J., Asada, H., Aziz, F., Kudo, F. A. and Sumpio, B. E. (2005). Differential effects of orbital and laminar shear stress on endothelial cells. *J. Vasc. Surg.* **41**, 869-880.

dela Paz, N. G., Walshe, T. E., Leach, L. L., Saint-Geniez, M. and D'Amore, P. A. (2012). Role of shear-stress-induced VEGF expression in endothelial cell survival. *J. Cell Sci.* **125**, 831-843.

Dolan, J. M., Kolega, J. and Meng, H. (2013). High wall shear stress and spatial gradients in vascular pathology: a review. *Ann. Biomed. Eng.* **41**, 1411-1427.

Dupuis-Girod, S., Bailly, S. and Plauchu, H. (2010). Hereditary hemorrhagic telangiectasia: from molecular biology to patient care. *J. Thromb. Haemost.* **8**, 1447-1456.

Fernandez-Sanchez, M.-E., Brunet, T., Röper, J.-C. and Farge, E. (2015). Mechanotransduction's impact on animal development, evolution, and tumorigenesis. *Annu. Rev. Cell Dev. Biol.* **31**, 373-397.

Franco, C. A., Jones, M. L., Bernabeu, M. O., Geudens, I., Mathivet, T., Rosa, A., Lopes, F. M., Lima, A. P., Ragab, A., Collins, R. T. et al. (2015). Dynamic endothelial cell rearrangements drive developmental vessel regression. *PLoS Biol.* **13**, e1002125.

Franco, C. A., Jones, M. L., Bernabeu, M. O., Vion, A.-C., Barbacena, P., Fan, J., Mathivet, T., Fonseca, C. G., Ragab, A., Yamaguchi, T. P. et al. (2016). Non-canonical Wnt signalling modulates the endothelial shear stress flow sensor in vascular remodelling. *eLife* **5**, e07727.

Givens, C. and Tzima, E. (2016). Endothelial mechanosignaling: does one sensor fit all? *Antioxid. Redox Signal.* **25**, 373-388.

Hahn, C. and Schwartz, M. A. (2009). Mechanotransduction in vascular physiology and atherogenesis. *Nat. Rev. Mol. Cell Biol.* **10**, 53-62.

Hajra, L., Evans, A. I., Chen, M., Hyduk, S. J., Collins, T. and Cybulsky, M. I. (2000). The NF-kappa B signal transduction pathway in aortic endothelial cells is primed for activation in regions predisposed to atherosclerotic lesion formation. *Proc. Natl. Acad. Sci. USA* **97**, 9052-9057.

Jin, Y., Muhl, L., Burmakin, M., Wang, Y., Duchez, A.-C., Betsholtz, C., Arthur, H. M. and Jakobsson, L. (2017). Endoglin prevents vascular malformation by regulating flow-induced cell migration and specification through VEGFR2 signalling. *Nature* **19**, 639-652.

Krause, C., Guzman, A. and Knaus, P. (2011). Noggin. *Int. J. Biochem. Cell Biol.* **43**, 478-481.

Larrivée, B., Prahst, C., Gordon, E., del Toro, R., Mathivet, T., Duarte, A., Simons, M. and Eichmann, A. (2012). ALK1 signaling inhibits angiogenesis by cooperating with the notch pathway. *Dev. Cell* **22**, 489-500.

Laux, D. W., Young, S., Donovan, J. P., Mansfield, C. J., Upton, P. D. and Roman, B. L. (2013). Circulating Bmp10 acts through endothelial Alk1 to mediate flow-dependent arterial quiescence. *Development* **140**, 3403-3412.

Li, J., Hou, B., Tumova, S., Muraki, K., Bruns, A., Ludlow, M. J., Sedo, A., Hyman, A. J., McKeown, L., Young, R. S. et al. (2014). Piezo1 integration of vascular architecture with physiological force. *Nature* **515**, 279-282.

McDonald, J., Wooderchak-Donahue, W., VanSant Webb, C., Whitehead, K., Stevenson, D. A. and Bayrak-Toydemir, P. (2015). Hereditary hemorrhagic telangiectasia: genetics and molecular diagnostics in a new era. *Front. Genet.* **6**, 1.

Moya, I. M., Umans, L., Maas, E., Pereira, P. N. G., Beets, K., Francis, A., Sents, W., Robertson, E. J., Mummery, C. L., Huylebroeck, D. et al. (2012). Stalk cell phenotype depends on integration of Notch and Smad1/5 signaling cascades. *Dev. Cell* **22**, 501-514.

Nakashima, Y., Plump, A. S., Raines, E. W., Breslow, J. L. and Ross, R. (1994). ApoE-deficient mice develop lesions of all phases of atherosclerosis throughout the arterial tree. *Arterioscler. Thromb.* **14**, 133-140.

Park, S. O., Wankhede, Z., Lee, Y. J., Fliess, N., Choe, S. W., Oh, S. H., Walter, G., Raizada, M. K., Sorg, B. S., Oh, S. P. (2009). Real-time imaging of de novo arteriovenous malformation in a mouse model of hereditary hemorrhagic telangiectasia. *J. Clin. Invest.* **119**, 3487-3496.

Development (2017) 144, 3241-3252 doi:10.1242/dev.150904

Ranade, S. S., Qiu, Z., Woo, S.-H., Hur, S. S., Murthy, S. E., Cahalan, S. M., Xu, J., Mathur, J., Bandell, M., Coste, B. et al. (2014). Piezo1, a mechanically activated ion channel, is required for vascular development in mice. *Proc. Natl. Acad. Sci. USA* **111**, 10347-10352.

Rochon, E. R., Menon, P. G. and Roman, B. L. (2016). Alk1 controls arterial endothelial cell migration in lumenized vessels. *Development* **143**, 2593-2602.

Roman, B. L. and Pekkan, K. (2012). Mechanotransduction in embryonic vascular development. *Biomech. Model. Mechanobiol.* **11**, 1149-1168.

Sato, Y., Poynter, G., Huss, D., Filla, M. B., Czirok, A., Rongish, B. J., Little, C. D., Fraser, S. E. and Lansford, R. (2010). Dynamic analysis of vascular morphogenesis using transgenic quail embryos. *PLoS ONE* **5**, e12674.

Sorensen, L. K., Brooke, B. S., Li, D. Y. and Urness, L. D. (2003). Loss of distinct arterial and venous boundaries in mice lacking endoglin, a vascular-specific TGFbeta coreceptor. *Dev. Biol.* **261**, 235-250.

Sugden, W. W., Meissner, R., Aegerter-Wilmsen, T., Tsaryk, R., Leonard, E. V., Bussmann, J., Hamm, M. J., Herzog, W., Jin, Y., Jakobsson, L. et al. (2017). Endoglin controls blood vessel diameter through endothelial cell shape changes in response to haemodynamic cues. *Nat. Cell Biol.* **19**, 653-665.

Tual-Chalot, S., Oh, S. P. and Arthur, H. M. (2015). Mouse models of hereditary hemorrhagic telangiectasia: recent advances and future challenges. *Front. Genet.* **6**, 25.

Tzima, E., Del Pozo, M. A., Kiosses, W. B., Mohamed, S. A., Li, S., Chien, S. and Schwartz, M. A. (2002). Activation of Rac1 by shear stress in endothelial cells mediates both cytoskeletal reorganization and effects on gene expression. *EMBO J.* **21**, 6791-6800.

Tzima, E., Irani-Tehrani, M. and Kiosses, W. (2005). A mechanosensory complex that mediates the endothelial cell response to fluid shear stress. *Nature* **437**, 426-431.

Udan, R. S., Vadakkan, T. J. and Dickinson, M. E. (2013). Dynamic responses of endothelial cells to changes in blood flow during vascular remodeling of the mouse yolk sac. *Development* **140**, 4041-4050.

Wang, C., Baker, B. M., Chen, C. S. and Schwartz, M. A. (2013). Endothelial cell sensing of flow direction. *Arterioscler. Thromb. Vasc. Biol.* **33**, 2130-2136.

Wang, S., Helker, C. S. M., Rasouli, S. J., Maischein, H.-M., Offermanns, S., Herzog, W., Kwon, H.-B. and Stainier, D. Y. R. (2016). In vivo modulation of endothelial polarization by Apelin receptor signalling. *Nat. Commun.* **7**, 1-12.

Xu, C., Hasan, S. S., Schmidt, I., Rocha, S. F., Pitulescu, M. E., Bussmann, J., Meyen, D., Raz, E., Adams, R. H. and Siekmann, A. F. (2014). Arteries are formed by vein-derived endothelial tip cells. *Nat. Commun.* **5**, 5758.

Zhou, J., Lee, P.-L., Tsai, C.-S., Lee, C.-I., Yang, T.-L., Chuang, H.-S., Lin, W.-W., Lin, T.-E., Lim, S. H., Wei, S.-Y. et al. (2012). Force-specific activation of Smad1/5 regulates vascular endothelial cell cycle progression in response to disturbed flow. *Proc. Natl. Acad. Sci. U.S.A.* **109**, 7770-7775.

Zudaire, E., Gambardella, L., Kurcz, C. and Vermeren, S. (2011). A computational tool for quantitative analysis of vascular networks. *PLoS ONE* **6**, e27385.

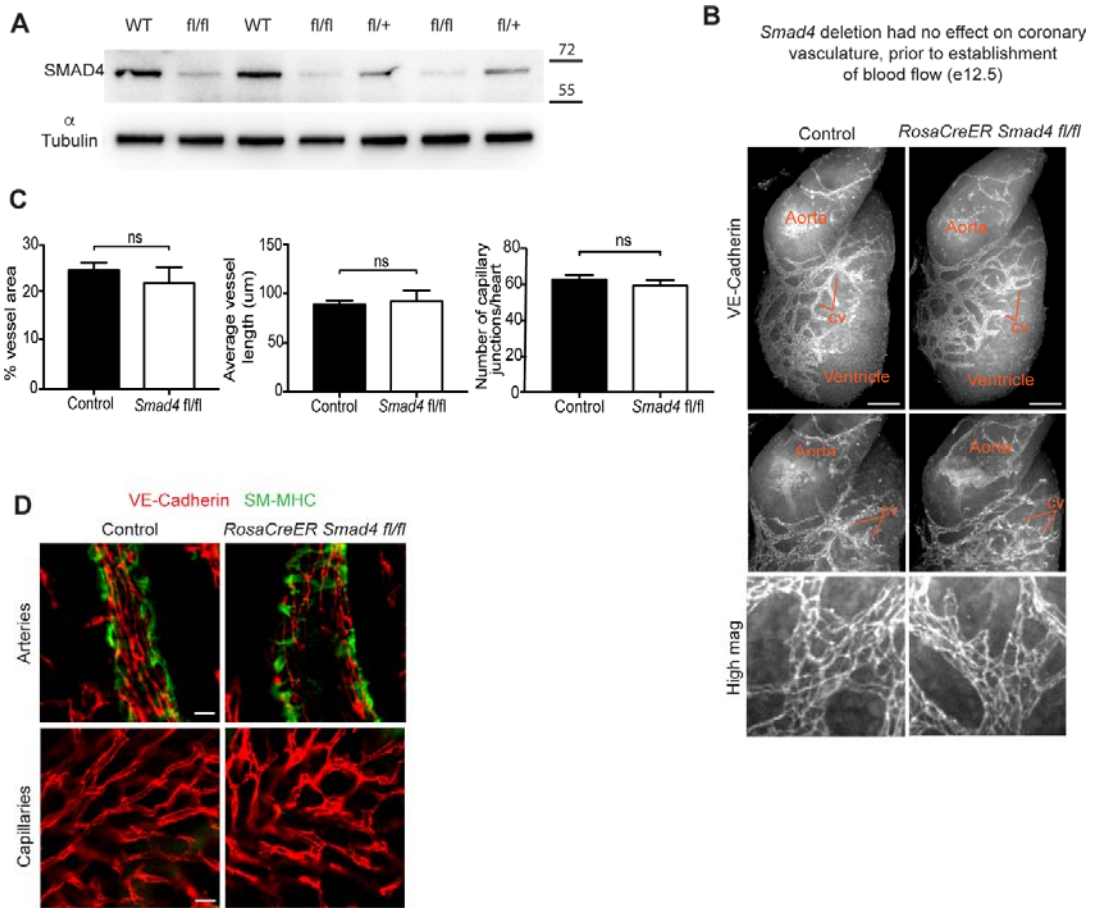

Figure S1. Vessel phenotypes in *Smad4* deficient mice. (A) Western analysis of SMAD4 is embryo lysates shows a dose dependent depletion of SMAD4 in wild type, *Smad4 fl/+,* and *Smad4 fl/fl* animals. (B) Imaging of e12.5 *RosaCre Smad4 floxed* animals. The coronary vascular plexus, including peritruncal vessels near the aorta, is comparable between mutant and control animals at e12.5, prior to blood flow. (C) Quantification of peritruncal vessel parameters (Controls: n=4 and *RosaCreER Smad4* fl/fl: n=5).(D) Imaging of high magnification of arteries and capillaries at e15.5. Error bars are s.d. ns, non-significant. Cv, coronary vessels, Scale bars, B ,100 μm and D, 50 μm.

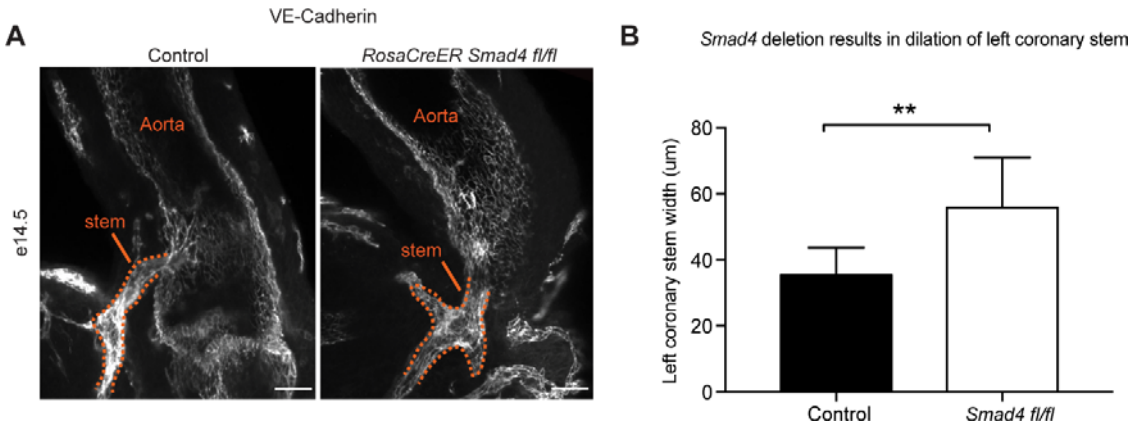

Figure S2. The left coronary artery stem is dilated in *Smad4* mutants. (A) Confocal image of a left coronary artery stem in a control and mutant heart. (B) Quantification of stem width (Controls: n=8 and *RosaCreER Smad4* fl/fl: n=8). Error bars are s.d. **, p≤0.01. Scale bars, A, 50 μm.

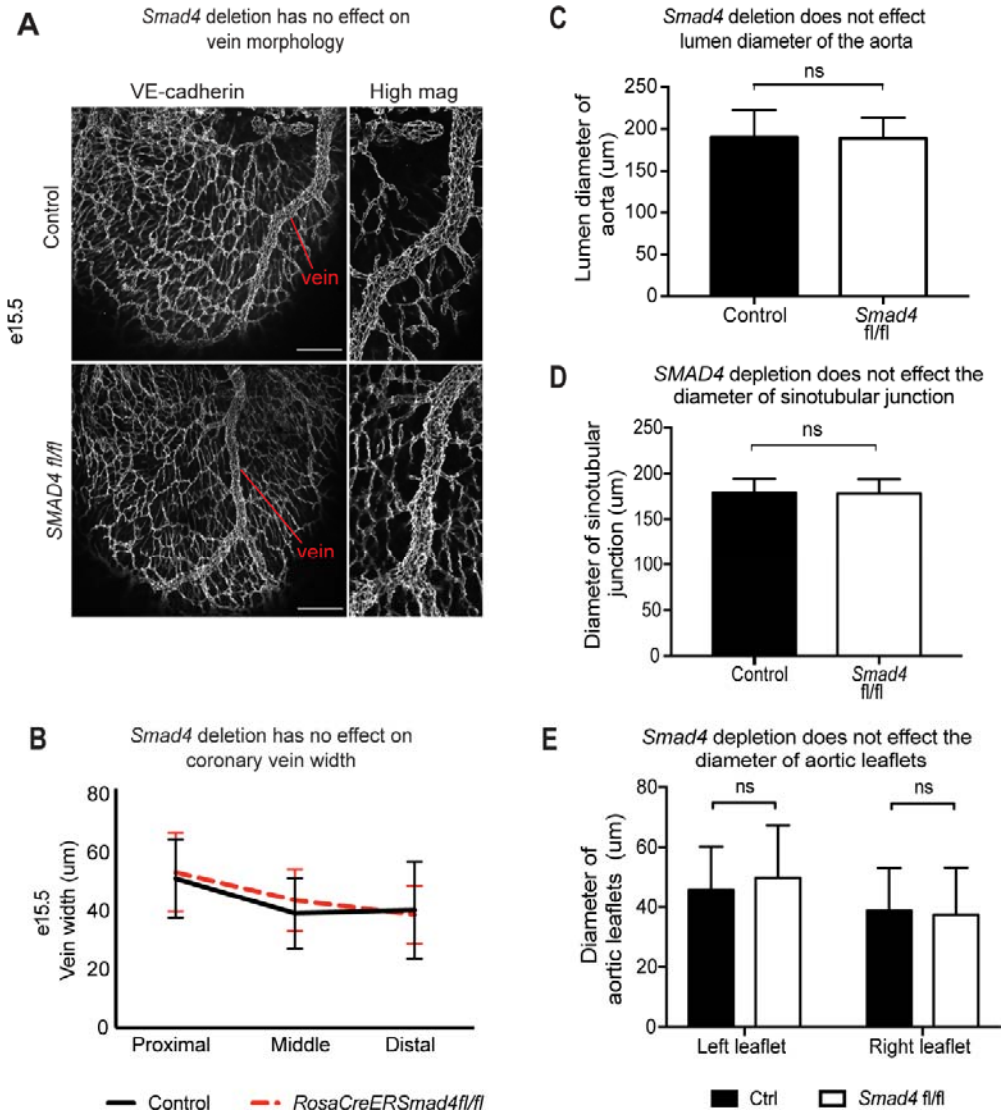

Figure S3. Various cardiac structures with no defects in *Smad4* mutants. (A and B) Confocal images (A) and quantification (B) of coronary veins (Controls: n=7 and *RosaCreER Smad4* fl/fl: n=8). (C-D) Measurements of the outflow tract (Controls: n=9 and *RosaCreER Smad4* fl/fl: n=10). Error bars are s.d. ns, non-significant. Scale bars, A, 100 μm.

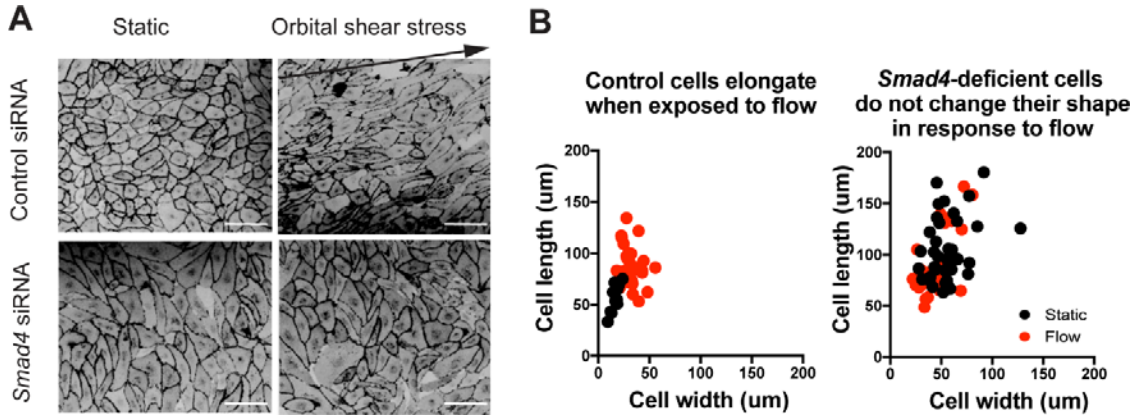

Figure S4. Alignment of *Smad4*-deficient cells in response to shear stress imparted by orbital flow. (A and B) Human coronary artery endothelial cells (HCAECs) exposed to orbital laminar shear stress (arrow indicates direction). (A) Cell-cell junctions are immunostained with VE-cadherin (black) showing the absence of alignment with flow when treated with *Smad4* siRNA. (B) The absence of shear stress-induced cell shape change is quantified by plotting cell length versus width. Each dot is an individual cell. Scale bar, 50 μm.

Movie S1. Endothelial cells treated with control siRNA align and migrate against the direction of flow. Time-lapse movie (1 frame every 15 minutes) of HCAECs treated with control siRNA subjected to shear stress at 35 dyne/cm^2 for 72 hours. The direction of flow is left to right.

Movie S2. Endothelial cells treated with *Smad4* siRNA do not align and migrate against the direction of flow. Time-lapse movie (1 frame every 15 minutes) of HCAECs treated with *Smad4*-targeted siRNA subjected to shear stress at 35 dyne/cm^2 for 72 hours. The direction of flow is left to right.